

# BOGOLIUBOV LABORATORY OF THEORETICAL PHYSICS

At the Bogoliubov Laboratory of Theoretical Physics (BLTP), studies are carried out on the following four themes: Fields and Particles, Modern Mathematical Physics, Nuclear Theory, and Theory of Condensed Matter. Important components of BLTP's activities

are theoretical support of experimental research to be carried out with JINR's participation and recruiting of young researchers, students, and post-graduate students to the Laboratory.

## FIELDS AND PARTICLES

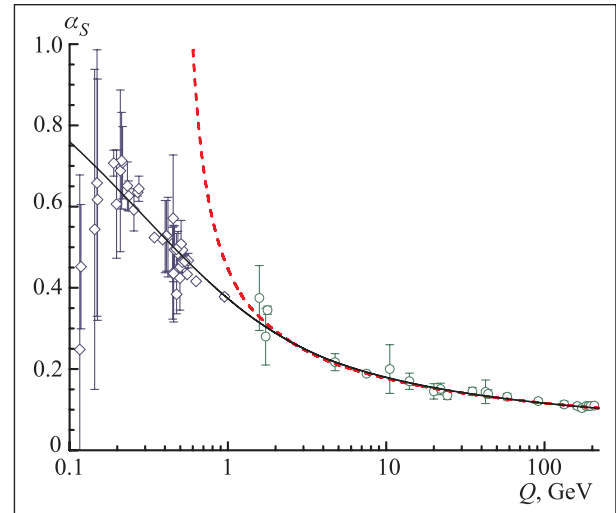
Theoretical investigations in the Theory of Fields and Particles were continued in the framework of the following projects:

- Standard model and its extensions;
- QCD parton distributions for modern and future colliders;
- Physics of heavy and exotic hadrons;
- Mixed phase in heavy-ion collisions.

Last year, considerable progress was achieved in several directions. Below one can find a brief description of the selected results obtained at BLTP in 2007.

The strong running coupling  $\alpha_s(Q^2)$  was studied in the low-energy domain below 1 GeV. To this end, the combination of the three-dimensional Bethe–Salpeter (BS) formalism for a quark–antiquark system with the analytic perturbation theory (APT) algorithm was employed. This combined BS+APT approach enables one to extract values of  $\alpha_s(Q^2)$  for the momentum transferred  $Q$  range between 200 MeV and 1 GeV. The extracted values agree with the APT curve normalized at its current world average value  $\alpha_s(M_Z^2) \approx 0.118$ , see the Figure. This indicates that an analytic-type modification of perturbative QCD at low energies has a chance for providing one with a theoretically consistent and numerically correct description of hadron physics in the energy range from a few hundred MeV up to a few hundred GeV [1].

The validity of the recently proposed asymptotic Bethe ansatz at weak coupling was verified by comparing the Bethe ansatz predictions for the four-loop



Summary of BS+APT extracted ( $\diamond$ ) and high-energy ( $\circ$ ) data for  $\alpha_s(Q^2)$  against the three-loop analytic running coupling (solid curve), and its perturbative counterpart (dashed curve), both normalized at the  $Z_0$ -boson mass

anomalous dimension of finite-spin twist-two operators to Balitsky–Fadin–Kuraev–Lipatov (BFKL) constraints from high-energy scattering amplitudes in the  $N = 4$  gauge theory. It was found that the ansatz breaks down for twist-two operators at four-loop order. The exact form of four-loop anomalous dimension of the family of twist-two operators, which includes the Konishi field, was conjectured by introducing a contribution of wrap-

ping effects in agreement with BFKL predictions and double-logarithmic resummation [2].

It is shown that within the framework of the Minimal Supersymmetric Standard Model (MSSM) with the gravity-mediated soft supersymmetry breaking mechanism there exists an interesting possibility of getting long-lived next-to-lightest supersymmetric particles. There might be light superpartners of tau-leptons (staus) in the so-called coannihilation region of the MSSM parameter space. The region with large negative values of the trilinear soft supersymmetry breaking parameter  $A$  is distinguished by light superpartners of top-quarks (stops). Their production cross sections crucially depend on a single parameter, the mass of the superparticle, and for light staus can reach a few per cent of pb. This is within the reach of Large Hadronic Collider (LHC). The stop production cross section achieves tens or even hundreds pb for the stop mass around 150–200 GeV. Decays of long-living staus and stops would have an unusual signature if heavy charged particles decay with a considerable delay in secondary vertices inside the detector, or even escape the detector. Both regions are consistent with experimental Higgs and chargino mass limits as well as with WMAP relic density limit [3].

High precision theoretical predictions for processes to be investigated at LHC were obtained. In particular, radiative corrections to Drell–Yan-like processes (single  $Z$ - and  $W$ -boson production) were evaluated. Complete one-loop electroweak radiative corrections to the differential distribution of semileptonic top-quark decays were presented for the first time. For the conditions of the COMPASS experiment at CERN, one-loop corrections to the leptonic tensor in bremsstrahlung of high-energy leptons on heavy nuclei were calculated [4].

The cross section for polarized and unpolarized electron–proton scattering was calculated by taking into account radiative corrections in the leading and next-to-leading logarithmic approximation. The expression of the cross section is formally similar to the cross section of the Drell–Yan process, where the structure functions of the electron play the role of the Drell–Yan probability distributions. The interference of the Born amplitude with the two-photon exchange amplitude (box-type diagrams) is expressed as a contribution to the  $K$  factor. It is calculated under the assumption that proton form factors decrease rapidly with the momentum transfer squared and that the momentum is equally shared between the two photons. The calculation of the box amplitude is done when the intermediate state is the proton or the Delta resonance. The results of numerical estimations show that the present calculation of radiative corrections can bring into agreement the conflicting experimental results on proton electromagnetic form factors and that the two-photon contribution is very small [5].

The analytic properties of the zero-angle scattering  $ep \rightarrow ep$  amplitude were used to derive the sum rules which connect the proton form factors with the differential cross section of inelastic  $ep \rightarrow eX$  diffractive scattering. The case of small momentum transfer connects the radii and anomalous magnetic moments with the photoproduction cross section without rapidity gaps in the final state [6].

The analytical properties of the hard exclusive process amplitudes were studied. The QCD factorization for deeply virtual Compton scattering and hard exclusive vector-meson production results in the subtracted dispersion relation with the subtraction constant determined by the Polyakov–Weiss  $D$  term. The continuation to the real photon limit is considered and the numerical correspondence between lattice simulations of the  $D$  term and the low-energy Thomson amplitude is found. For sufficiently large  $t$  the subtraction may be expressed in the form similar to that suggested earlier for real Compton scattering [7].

The general formulae connecting the structure functions  $W_i$  for quasi-elastic neutrino and antineutrino scattering off nucleons with the hadronic-current form factors, which take into account the final lepton mass, proton–neutron mass difference, and nonstandard ( $G$ -parity violating) second-class currents, were derived. Within the framework of the relativistic Fermi gas model by Smith and Moniz, the nuclear structure functions  $T_i$  were obtained which take into account the Fermi motion, Pauli blocking effects, and binding energy for nuclear targets. A statistical analysis of all available accelerator data on the total and differential cross sections as well as the  $Q^2$  distributions of events for quasi-elastic scattering of muon neutrino and antineutrino on hydrogen, deuterium, carbon, argon, iron, propane, freon, propane–freon mixture, and neon–hydrogen mixture was performed. The vector form factors  $G_E^p, G_M^p, G_E^n, G_M^n$  were evaluated on the basis of the phenomenological model, which describes well the experimental results extracted from the  $ep$ -scattering data. Within the standard assumptions, the world-averaged value of the axial mass of the nucleon  $M_A = (1.01 \pm 0.01) \text{ GeV}/c^2$  was obtained. This value does not contradict the preliminary result of the NOMAD experiment  $((1.05 \pm 0.02 \pm 0.07) \text{ GeV}/c^2$  for neutrino–carbon sample and  $(1.06 \pm 0.07 \pm 0.12) \text{ GeV}/c^2$  for antineutrino–carbon sample), but hardly hitch the results of the recent experiments K2K and MiniBooNE reporting 20% higher values of the axial mass [8].

The thermal and quark/baryon chemical potential dependences of quark condensate and masses of  $\pi$  and  $\sigma$  mesons were studied in the instanton model of the QCD vacuum in precritical region. The impact of phonon-like excitations of instanton liquid on the characteristics of  $\sigma$  meson in such an environment was also examined [9].

In the dispersive approach to the amplitude of the rare decay  $\pi^0 \rightarrow e^+e^-$ , the nontrivial dynamics is con-

tained only in the subtraction constant. In the leading order in  $(m_e/\Lambda)^2$  perturbative series, this constant was expressed in terms of the inverse moment of the pion transition form factor given in symmetric kinematics. In asymmetric kinematics, the lower bound of the de-

cay branching ratio was found using the CELLO and CLEO data on the pion transition form factor. The QCD restrictions lead to the quantitative prediction for the branching  $B(\pi^0 \rightarrow e^+e^-) = (6.2 \pm 0.1) \cdot 10^{-8}$  which is  $3\sigma$  below the recent KTeV measurement [10].

## MODERN MATHEMATICAL PHYSICS

Below, we present selected results obtained in 2007. The topics of main focus in the theme were:

- Supersymmetry and superstrings;
- Quantum groups and integrable systems;
- Quantum gravity and cosmology.

The Feynman path integral technique was applied to investigate superintegrable systems on two-dimensional spaces of nonconstant curvature, the Darboux spaces  $D_I-D_{IV}$ . The path integrals, in separating coordinate systems, were evaluated and led to explicit expressions for the Green functions, the discrete and continuous wave functions, and the discrete energy-spectra [11].

The integrable open chain models of  $gl(n|m)$  type are formulated in terms of the generators of the affine Hecke algebra. The hierarchy of commutative elements (which are analogs of the commutative higher integrals of motions) was constructed, and a set of functional equations for these elements was found [12].

The method of projection for the construction of vectors in the space of states of the quantum integrable models was formulated and compared with the nested Bethe ansatz. Universal Bethe equations were obtained. This allows one to unify the hierarchical and analytical Bethe ansatz in a unique theory which describes universal properties of the space of states in the quantum integrable models associated with the algebras  $gl_N$  [13].

It was demonstrated that eigenvalues of the family of Baxter  $Q$ -operators for supersymmetric integrable spin chains constructed with the  $gl(K|M)$ -invariant  $R$ -matrix obey the Hirota bilinear difference equation. The nested Bethe ansatz for superspin chains, with any choice of a simple root system, was then treated as a discrete dynamical system for zeros of polynomial solutions to the Hirota equation. The basic tool used was a chain of Backlund transformations for the Hirota equation connecting quantum transfer matrices. This approach also provides a systematic way to derive a complete set of generalized Baxter equations for superspin chains [14].

In view of a formulation of the Mirror Symmetry Conjecture for Fano varieties given by Hori and

Vafa, the Lagrangian tori for the projective plane and other toric Fano varieties were studied. It was established that the Hori–Vafa conjecture can be formulated in terms of the Bohr–Sommerfeld conditions, which implies a relationship between Mirror Symmetry and Geometric Quantization in terms of the Lagrangian geometry [15].

A new model of  $N = 8$  superconformal mechanics was proposed. It is associated with the action of a self-interacting off-shell  $N = 8$  multiplet  $(\mathbf{1}, \mathbf{8}, \mathbf{7})$  and, surprisingly, respects the invariance under the exceptional  $N = 8, d = 1$  superconformal group  $F(4)$  with the  $R$ -symmetry subgroup  $SO(7)$  [16].

The study of theories in superspaces with nonanticommutative deformations was continued. It was shown that though the NAC-deformed theories in the Minkowski superspaces lead to non-Hermitian Hamiltonians  $H$ , the latter can be made manifestly Hermitian via the similarity transformation  $H \rightarrow e^R H e^{-R}$  with a proper  $R$  [17].

A new nonlinear off-shell one-dimensional  $N = 8$  supermultiplet with three bosonic and eight fermionic physical degrees of freedom was revealed and studied. The geometry of the action of the relevant supersymmetric mechanics is specified by a function obeying the three-dimensional Laplace equation on the sphere  $S^3$  [18].

The recently obtained relation between static states, cosmologies, and waves was extended to a new class of integrable two-dimensional dilaton gravity theories in which scalar matter satisfies the Toda equations. The simplest cases of the Toda system are considered in detail and it is shown how the wave-like solutions of the general Toda systems can be simply derived. In the dilaton gravity theory these solutions describe nonlinear waves coupled to gravity [19].

It was demonstrated that all supergravity billiards corresponding to sigma-models on any  $U/H$  noncompact-symmetric space and obtained by compactifying supergravity to  $D = 3$  are fully integrable. The key point in establishing the integration algorithm is provided by an upper triangular embedding of the solvable Lie algebra associated with  $U/H$  into  $SL(N, R)$  which always exists. In this context, a remarkable re-

lation between the arrow of time and the properties of the Weyl group was established. The asymptotic states of the developing Universe are in the one-to-one correspondence with the elements of the Weyl group which is a property of the Tits–Satake universality classes and not of their single representatives. Furthermore, the Weyl group admits a natural ordering in terms of  $L(T)$ , the number of reflections with respect to the simple roots. The direction of time flows is always towards increasing  $L(T)$  which unexpectedly plays the role of an entropy [20].

According to the concept of gravity as an emergent phenomenon, the space-time metric is an effective low-energy variable and metric changes are collective excitations of underlying degrees of freedom of some unknown fundamental theory. In this approach the properties of the entropy of entanglement  $S$  between the fundamental degrees of freedom spatially divided by a surface were investigated [21].

When looking for physically viable theories at Planck scales the idea of noncommuting coordinates is widely used now. Interactions of noncommutative waves and solitons in  $2 + 1$  dimensions were analyzed exactly for a supersymmetric and integrable  $U(n)$  chiral model extending the Ward model. Explicit time-dependent solutions of its noncommutative field equations were constructed via iterative solving of linear equations. The approach was illustrated by presenting scattering configurations for two noncommutative  $U(2)$  plane waves and for two noncommutative  $U(2)$  solitons as well as by producing a noncommutative  $U(1)$  two-soliton bound state [22].

The problem of gravitational singularity also attracts attention of researchers. The viability of the vacuum Gauss–Bonnet cosmology was analyzed by examining the dynamics of the homogeneous and anisotropic background in  $4 + 1$  dimensions. The trajectories of the system originate either from the standard singularity or from nonstandard type, the later is characterized by the divergence of time derivative of the Hubble parameters for its finite value. At the onset, the system should

relax to the Einstein phase at later times as the effect of the Gauss–Bonnet term becomes negligible in the low-energy regime. However, it was found that most of the trajectories emerging from the standard Big-Bang singularity lead to future recollapse whereas the system beginning its evolution from the nonstandard singularity enters the Kasner regime at later times. This leads to the conclusion that the measure of trajectories giving rise to a smooth evolution from a standard singularity to the Einstein phase is negligibly small for generic initial conditions [23].

Powerful methods in observational astronomy are provided by making use of gravitation lensing. In particular, the application of gravitation lensing in the Röntgen and radio bands was considered for detecting the nearest massive black holes in our Galactic. It is shown that the approximation of a strong gravitation field should be used in this approach [24].

A number of rather sophisticated mathematical methods are widely used in studies aimed at extension of gravitation theories. The spectral analysis of differential operators is one of these methods. It was shown explicitly that in dynamics of theories with higher derivatives there arises exponential instability with respect to an external dissipative force. This fact should be taken into account in any extension of standard field theory models by making use of higher derivatives [25].

The spectral summation technique was applied in Casimir studies which are very urgent now in view of their relevance to nanophysics and nanotechnology. The Casimir force which attracts the slabs of finite thickness made of intrinsic and doped silicon with different concentration of carriers was calculated and the results were compared to those obtained for gold slabs. The Drude and the plasma models were used to describe the dielectric function for the carriers in doped Si. The conditions for getting the Casimir repulsion between two nonequal plates was also analyzed [26].

## NUCLEAR THEORY

In 2007, investigations were carried out in accordance with the four projects:

- Nuclear structure far from the valley of stability;
- Nucleus–nucleus interactions and nuclear properties at low excitation energies;
- Exotic few-body systems;
- Nuclear structure and dynamics at relativistic energies.

The distributions of dipole strength in tin isotopes were

studied. The calculations were performed within the Quasiparticle Random Phase Approximation using the separabilized Skyrme interactions of the three types of parameterizations SLy4, SkM\*, and SIII. The low-lying part of dipole strength distribution reveals the existence of a group of slightly collective states and the corresponding  $E1$  transition strength increases with the enlargement of neutron excess. The group is associated with the Pygmy resonance [27].

Experimental data for the energies and  $E2$  reduced transition probabilities for the  $2_1^+$  and  $2_{\gamma(\beta)}^+$  states in strongly deformed axially symmetric nuclei were analyzed with the collective Bohr Hamiltonian. It was shown that the mass coefficients for the  $\gamma(\beta)$ -vibrational motion and rotational motion are significantly different and their ratio extracted from the experimental data takes the values in the range 3–5. The nuclei in the middle of the rare-earth region, which are axially symmetric and have small fluctuations in  $\beta$  and  $\gamma$ , can be described correctly with a form of Bohr Hamiltonian with different but constant values for mass coefficients for the ground,  $\beta$  and  $\gamma$  bands. An inclusion into consideration of not only scalar but also other components of the mass tensor can explain the difference in the values of the mass coefficients for the  $\gamma(\beta)$  vibrations and the ground-state rotations [28].

The large amplitude isoscalar and isovector deformation properties of the neutron-rich isotope  $^{20}\text{O}$  were investigated by means of Hartree–Fock–Bogoliubov calculations with independent constraints on axial neutron and proton quadrupole moments  $Q_n$  and  $Q_p$ . Using the particle-number and angular-momentum projected generator coordinate method the collective dynamics in the  $\{\langle Q_n \rangle, \langle Q_p \rangle\}$  plane was analyzed. It was found that already for this moderately neutron-rich nucleus the transition moments are modified when independent neutron and proton collective dynamics are allowed [29].

A shape evolution of  $^{162,164}\text{Yb}$  in yrast states was studied by using the self-consistent Skyrme–Hartree–Fock calculations. It was found that nonaxial octupole deformations become favorable at  $\hbar\Omega > 0.4$  MeV in  $^{162}\text{Yb}$ , while in  $^{164}\text{Yb}$  a nonaxial quadrupole shape is dominant at fast rotation. At  $\hbar\Omega \approx 0.45$  MeV the octupole phonon solution vanishes in the rotating frame in  $^{162}\text{Yb}$ . It results in the onset of the degeneracy between the lowest negative parity and negative signature band, and the positive parity and positive signature yrast line. This explains the spontaneous breaking of reflection symmetry of the rotating mean field. In contrast, in  $^{164}\text{Yb}$  the octupole correlations manifest themselves as low-lying octupole vibrations of the quadrupole deformed rotating nucleus [30].

The generation of sizable angular momenta in fragments formed in low-energy nuclear fission was described microscopically within the general quantum-mechanical framework of orientation pumping due to the Heisenberg uncertainty principle. Within this framework, the results of Skyrme–Hartree–Fock plus BCS-pairing calculations of fragment deformabilities to deduce a distribution of fission-fragment spins as a function of the fragment total excitation energy, were used. Particular attention was paid to quantitatively defining the scission configurations and to studying various implications of such a specific choice. Fair qualitative agreement with data on spon-

taneous fission  $^{252}\text{Cf} \rightarrow ^{106}\text{Mo} + ^{146}\text{Ba}$  was demonstrated [31].

The induced nuclear fission was considered as a transport process over the fission barrier underlying dissipative forces. Using a quantum master equation for the reduced density matrix, the influence of microscopic diffusion coefficients on the total fission time and transient time was studied. In the quantum case, the transient times appear to be larger by a factor of about 2 than those in the classical case based on the Langevin equation. At moderate to high excitation energies the asymptotic fission rates in the classical and quantum cases are almost the same. At the friction coefficient  $\hbar\lambda_p \approx 1$  MeV the transient time changes from  $10^{-21}$  to  $4 \cdot 10^{-21}$  s with decreasing temperature from  $T = 5$  MeV to  $T = 0.7$  MeV. At the same time, the fission lifetime changes from  $10^{-21}$  to  $5.4 \cdot 10^{-19}$  s. The main contribution to the fission time comes from the time spent by the fissioning nucleus before the saddle point [32].

The neutron emission from the Dinuclear System (DNS), being in the local potential minimum and formed in the entrance channel of the reactions  $^{62-73}\text{Ni} + ^{208}\text{Pb}$ , was studied using the statistical approach. The probability of neutron emission from the DNS is found to be of an order of  $10^{-2}$  and increases by a factor of 3 with the DNS mass number from 270 to 281. This increase occurs slower than in the compound nucleus. The process which mainly competes with the pre-scission neutron emission in Pb-based reactions is the quasifission from the initial DNS and more symmetrical DNS. The study of the neutron emission from the DNS makes it possible to find out whether the neck growth is a fast or slow process in the DNS. The neutron emission decreases the excitation energy of the DNS and, therefore, could help produce almost cold and relatively long-lived DNS which can be interpreted as hyperdeformed nuclear states [33].

The experimental cross sections of elastic proton scattering off the nucleus  $^6\text{He}$  measured at FLNR JINR and other laboratories were analyzed with the microscopic optical potential (OP) and model densities of the nucleus. The microscopic OP consists of the real folding potential and the imaginary part which is calculated using the high-energy approximation method. This OP has no free parameters and is determined by the nuclear density of  $^6\text{He}$ , the effective  $NN$  potential and the  $NN$  total cross section. Three current models of the  $^6\text{He}$  structure were tested. It was shown that the Large Scale Shell Model is preferable. Good agreement with the data was obtained at  $E > 40$  MeV/n [34].

Energy correlations in transitions from the bound state to the three-body continuum of Borromean halo nuclei were considered. A core +  $n + n$  three-body cluster model, which reproduces the experimentally known properties of  $^6\text{He}$  and  $^{11}\text{Li}$ , was used to study the low-lying resonances and soft modes. An analysis of the

correlated responses in  ${}^6\text{He}$  shows that in the case of the narrow three-body  $2_1^+$  resonance the transition energy correlations are the same as in the intrinsic correlated structure in  $3 \rightarrow 3$  scattering. They differ significantly for wide  $2_2^+$ ,  $1_1^+$  resonances, and also for the soft dipole and monopole modes, where, due to the transition operators, the intertwining of the ground state and the three-body continuum plays a significant role [35].

The standard model of the  $pp$ -cycle in the Sun assumes that the two binary reactions are responsible for the destruction of  ${}^7\text{Be}$ : a)  $e+{}^7\text{Be}={}^7\text{Li}+\nu$ ; b)  $p+{}^7\text{Be}={}^8\text{B}+\nu$ . The rates of these processes were studied under the assumption on the ternary mechanism of the electron capture in the solar media. With this aim, the expansion of the three-body continuum wave function in the small parameter  $(m_e/m_p)^{1/2}$ , where  $m_e(m_p)$  is the electron (proton) mass, is applied. Due to the influence of the proton as the third particle the electron capture rate by the  ${}^7\text{Be}$  nucleus increases and the destruction rate of  ${}^7\text{Be}$  nuclei is increased as well. This results in the decrease of the concentration of  ${}^8\text{B}$  nuclei in the Sun which are the source of high-energy solar neutrinos [36].

Several new optimal bounds on variation of spectra and spectral subspaces of a self-adjoint Hamiltonian under off-diagonal perturbations were established. In particular, it was proven that if the spectrum of the Hamiltonian consists of two disjoint components  $\sigma_0$  and  $\sigma_1$ , the gaps between them remain open whenever the norm of the perturbation  $V$  satisfies the bound  $\|V\| < d\sqrt{3/2}$ , where  $d = \text{dist}(\sigma_0, \sigma_1)$ . Furthermore, if the convex hull of the set  $\sigma_0$  does not intersect the set  $\sigma_1$ , then the perturbation  $V$  does not close the gaps between  $\sigma_0$  and  $\sigma_1$  under a much weaker condition  $\|V\| < d\sqrt{2}$ . Under the latter condition an extended version of the Davis–Kahan *a posteriori*  $\tan \Theta$  theorem for eigenspaces as well as the corresponding *a priori*  $\tan \theta$  theorem for eigenvectors were proven [37].

The universal three-body dynamics in ultra-cold binary Fermi and Fermi–Bose mixtures was studied. A comprehensive universal description of the rotational-vibrational spectrum for two identical particles of mass  $m$  and the third particle of mass  $m_1$  in the zero-range limit of the interaction between different particles was given for arbitrary values of the mass ratio  $m/m_1$  and the total angular momentum  $L$ . For those  $L$  and  $m/m_1$ , which correspond to the finite number of vibrational states, all the binding energies are described by the universal function depending on two scaled variables. In the case  $L = 1$ , a two-humped structure in the mass-ratio dependencies of the elastic scattering cross section and the three-body recombination rate is related to emerging of bound states [38].

The proposed earlier relativistic mean-field model with hadron masses and coupling constants depending

on the  $\sigma$ -meson field was generalized to finite temperatures. The in-medium behavior of the hadron masses motivated by the Brown–Rho scaling was simulated. The high-lying baryon resonances and boson excitations as well as excitations of the  $\sigma$ ,  $\omega$ , and  $\rho$  fields interacting via mean fields were incorporated into this scheme. It was demonstrated that EoS can be matched with that computed on the lattice for high temperatures provided the baryon resonance couplings with nucleon are partially suppressed. In this case, the quark liquid would masquerade as the hadron one. The model was applied to the description of heavy-ion collisions in a broad collision energy range. It might be especially helpful for studying a phase diagram in the region near possible phase transitions [39].

Asymmetry of the decay  $\omega \rightarrow e^+e^-$  in nuclear matter with respect to the electron and positron energies was investigated. The analysis was performed within a simple resonance model. It was shown that the excitation of high-spin resonances results in a strong momentum dependence of the asymmetry around mass of virtual  $\omega$  meson  $M = (0.75-0.8)$  GeV and it is flat at  $M = 0.7$  GeV. Thus, asymmetry is sensitive to the properties of the  $\omega$ -meson self-energy and may serve as a powerful tool in studying the properties of the  $\omega$  meson in the nuclear medium. Experimentally, the asymmetry can be studied at J-PARCE16, HADES at GSI (and later on at FAIR), CLAS G9 at JLab [40].

The electrodisintegration of a deuteron within the Bethe–Salpeter approach with a separable kernel of the nucleon–nucleon interaction was considered. This conception keeps the covariance of a description of the process. The reaction was investigated within the relativistic plane-wave impulse approximation. It was demonstrated that if the photon–neutron interaction is neglected, factorization of the cross section into photon–proton and spectator parts holds. The calculations performed for the cases both with and without the photon–neutron interaction show that the neutron plays an important role [41].

A possible modification of the wave function of the nucleon bound in a nucleus by the interaction with the surrounding medium was analyzed. It was argued that the modification should strongly depend on the momentum of the nucleon. The suppression of the point-like configurations of a nucleon bound in the nucleus  $A$  with the spectator nucleus  $A - 1$  being in a particular energy configuration was derived. It was shown that for nonrelativistic values of the nucleon momentum, the momentum dependence of the nucleon deformation appears to follow from rather general considerations. One more implication of the presented observations is a flattening of the  $A$  dependence of the EMC effect: very similar effects were obtained for  ${}^4\text{He}$  and  ${}^{12}\text{C}$  which agree well with the preliminary JLab data [42].

## THEORY OF CONDENSED MATTER

Theoretical investigations in the Theory of Condensed Matter were continued in the framework of the following projects:

- Physical properties of complex materials and nanostructures;
- Mathematical problems of many-particle systems.

A check of predictions of the logarithmic conformal field theory was undertaken. It is well known that the theory predicts logarithmic corrections to correlation functions for the models with the central charge  $c = -2$ , and gives numerical values of the coefficients at these corrections. However, there were no exact solutions up to now for the pair correlation functions containing logarithmic terms of leading orders. It was shown that the correlation functions containing the logarithmic terms appear in the Abelian ASM theory for the nonlocal operators. The ASM model belongs to the class of free-fermions models. The obtained correlation functions are in full agreement with the predictions of the logarithmic conformal theory [43].

The determinant expression for the time-dependent transition probabilities in the totally asymmetric exclusion process with parallel update on a ring was obtained. To this end, the method of summation over the roots of Bethe equations based on the multidimensional analogue of the Cauchy residue theorem was developed. This method was applied to construct the resolution of the identity operator from the generalized eigenvectors of the evolution operator, which were useful for calculation of the matrix elements of its powers. As a by-product, the generating function of the joint probability distribution of particle configurations and the total distance traveled by the particles were obtained [44].

One-dimensional Ising chains with nonlocal exchange, which are generated by particular self-similar infinite soliton solutions of the Korteweg–de Vries and B-type Kadomtsev–Petviashvili equations, were investigated. It is shown that in the scaling limit, when the interaction acquires a long-distance character, the effective temperature tends to zero and there appears a second order phase transition. In this case, the magnetization becomes a piecewise linear function of the external magnetic field and the magnetic susceptibility acquires a jump at the critical value of the magnetic field. Properties of solutions of the elliptic hypergeometric equation and the structure of multivariate elliptic hypergeometric functions of type I for the root system  $BC_n$  were investigated in detail [45].

The field emission of crystalline AAA graphite was studied within a simple analytical approach with account of the dispersion relation near the Fermi level. The emission current was calculated for two crystal orientations with respect to the applied electric field. It

was found that the band structure of the 3D graphite has had a marked impact on the field emission current. The exponent of the Fowler–Nordheim equation remains the same while the preexponential factor is markedly modified. For both field directions, the linear field dependence was found in weak fields. The standard quadratic Fowler–Nordheim behavior takes place in strong fields. A strong dependence of the emission current from the interlayer distance was observed. The known case of a single-walled carbon nanotube was also considered [46].

The recently proposed doped carrier Hamiltonian formulation of the  $t - J$  model is complemented with the constraint that projects out the unphysical states. With this new important ingredient, the previously used and seemingly different spin-fermion representations of the  $t - J$  model were shown to be gauge related to each other. This new constraint can be treated in a controlled way close to half-filling suggesting that the doped carrier representation provides an appropriate theoretical framework to address the  $t - J$  model in this region. This constraint also suggests that the  $t - J$  model can be mapped onto a Kondo–Heisenberg lattice model. Such a mapping highlights important physical similarities between the quasi two-dimensional heavy fermions and the high- $T_c$  superconductors. The physical implications of this model representation relate, in particular, the small versus large Fermi surface crossover to the closure of the lattice spin gap [47].

A model for two nondegenerate cavity fields coupled through a reservoir was exploited to describe Raman scattering in which the Stokes and anti-Stokes fields were produced. The phenomenon of entanglement between the Stokes and anti-Stokes fields was found due to their indirect interaction through the phonon bath and the strength of entanglement was evaluated depending on initial states of the fields and on a state of the phonon reservoir [48].

A microscopic theory of electronic spectrum and superconducting pairing within an effective  $p - d$  Hubbard model was developed. Exact Dyson equations for the normal and anomalous Green's functions were derived and solved in the noncrossing approximation for the matrix self-energy. Doping and temperature dependence of electron dispersions, spectral functions, the Fermi surface and doping dependence of the superconducting transition temperature were calculated. At low doping, an arc-type Fermi surface and a pseudogap in the spectral function were observed, which strongly suppresses superconducting  $T_c$  [49].

The McCumber–Steward dependence of the return current is generalized to the case of intrinsic Josephson junctions in high-temperature superconductors. The breakpoint current on the outermost branch was investi-

gated as a function of the coupling and dissipation parameters for stacks with a different number of junctions. The coupling and dissipation dependence of the break-point current is investigated and good qualitative agreement with the simulation results was obtained. The

commensurability effect is demonstrated and a collective behavior of the current-voltage characteristics for the stacks with a different number of junctions was predicted [50].

## DUBNA INTERNATIONAL ADVANCED SCHOOL OF THEORETICAL PHYSICS (DIAS-TH)

In 2007, the research-educational project DIAS-TH was successfully continued. The following activities in the framework of DIAS-TH took place: V Winter School on Theoretical Physics (January 28–February 6); XI Research Workshop «Nucleation Theory and Applications» (April 1–30); Helmholtz International School on Modern Mathematical Physics (July

22–30); Helmholtz International School «Nuclear Theory and Astrophysical Applications» (August 7–17); the regular seminars for students and post-graduates were organized; computer processing of video records of lectures was continued; Web-site of DIAS-TH was supported.

## COMPUTER FACILITIES

The powerful server purchased at the end of 2007 was brought into operation (dxcore.jinr.ru). Due to its two dual-core processors, 16 GB of 4-channel RAM subsystem and two fast hard disks, the new server shows performance about as big as combined performance of 4 dual-processor servers of the previous generation. The pool of personal computers at BLTP was

expanded by installation of 22 new machines. Most of them are equipped with dual-core processors which bring the power of multiprocessor calculations to desktop. Additional access points were installed in BLTP wireless network to improve connection quality and cover wider area.

## MEETINGS, SCIENTIFIC COLLABORATION

In 2007, besides the schools organized in the framework of DIAS-TH, the Laboratory participated in the organization of 7 international conferences and workshops held in Dubna and Prague:

- International workshop «Classical and Quantum Integrable Systems» (January 21–26, Dubna);
- International workshop «The Logarithmic Conformal Field Theories and Statistical Mechanics» (June 4–8, Dubna);
- XVI international colloquium «Integrable Systems and Quantum Symmetries» (June 14–16, Prague, Czech Republic);
- International conference «Muon Catalyzed Fusion and Related Topics» (June 18–21, Dubna);
- Advanced Study Institute «Symmetries and Spin» (July 8–14, Prague, Czech Republic);
- International workshop «Supersymmetries and Quantum Symmetries» (SQS'07) (July 30–August 4, Dubna);

- XII International workshop on High-Energy Spin Physics (September 3–7, Dubna).
- The workshop devoted to cooperation between the Asia Pacific Centre for Theoretical Physics (Korea) and Bogoliubov Laboratory of Theoretical Physics was held in Dubna (June 18–23, Dubna).

In 2007, the international collaboration was supported by grants of the plenipotentiaries of Bulgaria, the Czech Republic, Poland, the Slovak Republic, Hungary, Romania and the JINR Directorate; the collaboration with German theorists was based on the Heisenberg–Landau Programme; with Polish theorists, on the Bogoliubov–Infeld Programme; with Czech theorists, on the Blokhintsev–Votruba Programme; and Romanian theorists on the Titeica–Markov Programme.

Some studies were carried out in collaboration with scientists from Western Europe in the framework of the JINR–INFN, JINR–IN2P3 agreements and on the projects supported by INTAS, RFBR–DFG, RFBR–

CNRS. The agreement for collaboration between the Bogoliubov Laboratory and CERN TH is functioning.

## REFERENCES

1. *Baldicchi M. et al.* // Phys. Rev. Lett. 2007. V. 99. P. 242001.
2. *Kotikov A. V. et al.* // J. Stat. Mech. 2007. V. 0710. P. P10003.
3. *Gladyshev A. V., Kazakov D. I., Paucar M. G.* hep-ph/0710.2322v1; SUSY07 Proc. (submitted).
4. *Andonov A. et al.* // Part. Nucl. Lett. 2007. V. 4. P. 757; *Arbuzov A. et al.* // Europ. Phys. J. C. 2007. V. 51. P. 585; *Arbuzov A. B.* 0710.3639031. 2007; JHEP. 2008. 01 (submitted).
5. *Bystritskiy Yu. M., Kuraev E. A., Tomasi-Gustafsson E.* // Phys. Rev. C. 2007. V. 75. P. 015207.
6. *Dubnicka S., Dubnickova A. Z., Kuraev E. A.* // Phys. Rev. D. 2007. V. 75. P. 057901.
7. *Anikin I. V., Teryaev O. V.* // Phys. Rev. D. 2007. V. 76. P. 056007.
8. *Shirokov M. I., Naumov V. A.* // Concepts Phys. 2007. V. 4. P. 121; *Kuzmin K. S., Lokhtin K. S., Sinegovsky S. I.* // Phys. Part. Nucl. Lett. 2007. V. 4. P. 477.
9. *Molodtsov S. V. et al.* hep-ph/0702178. 2007.
10. *Dorokhov A. E., Ivanov M. A.* // Phys. Rev. D. 2007. V. 75. P. 114007.
11. *Grosche C., Pogosyan G. S., Sissakian A. N.* // Part. Nucl. 2007. V. 38, No. 3. P. 587.
12. *Isaev A. P.* // Theor. Mat. Phys. 2007. V. 150. P. 187.
13. *Enriquez B., Khoroshkin S., Pakuliak S.* // Commun. Math. Phys. 2007. V. 276. P. 691; *Khoroshkin S., Pakuliak S., Tarasov V.* // J. Geom. Phys. 2007. V. 57. P. 1713.
14. *Kazakov V., Sorin A. S., Zabrodin A.* // Nucl. Phys. B. 2008. V. 790. P. 345; hep-th/0703147.
15. *Tyurin N. A.* // Math. Soc. Lecture Notes. London. 2007. V. 338. P. 279; *Tyurin N. A.* // Teor. Math. Phys. 2007. V. 150. P. 325.
16. *Delduc F., Ivanov E.* // Phys. Lett. B. 2007. V. 654. P. 200.
17. *Ivanov E. A., Smilga A. V.* // JHEP. 2007. 0707. 036.
18. *Bellucci S., Krivonos S., Sutulin A.* // Phys. Rev. D. 2007. V. 76. P. 065017.
19. *Filippov A. T.* // Theor. Mat. Phys. 2007. V. 153. P. 422; *Filippov A. T.* hep-th/0801.1312. 2007.
20. *Fre P., Sorin A. S.* hep-th/0710.1059. 2007.
21. *Fursaev D.* hep-th/0711.1221. 2007.
22. *Gutschwager C., Ivanova T. A., Lechtenfeld O.* // J. High Energy Phys. 2007. V. 11. P. 052.
23. *Chingangbam R. et al.* hep-th/0711.2122. 2007.
24. *Barbashov B. M. et al.* // Phys. Atom. Nucl. 2007. V. 70. P. 191.
25. *Nesterenko V. V.* // Phys. Rev. D. 2007. V. 75. P. 087703.
26. *Lambrecht A. et al.* // Europhys. Lett. 2007. V. 77. P. 44006.
27. *Tarpanov D. et al.* // Phys. At. Nucl. 2007. V. 70. P. 1402.
28. *Jolos R. V., von Brentano P.* // Phys. Rev. C. 2007. V. 76. P. 024309.
29. *Severyukhin A. P. et al.* // Ibid. V. 75. P. 064303.
30. *Nazmitdinov R. G., Kvasil J., Tsvetkov A.* // Phys. Lett. B. 2007. V. 657. P. 159.
31. *Bonneau L., Quentin P., Mikhailov I. N.* // Phys. Rev. C. 2007. V. 75. P. 064313.
32. *Sargsyan V. V. et al.* // Ibid. V. 76. P. 064604.
33. *Zubov A. S. et al.* // Eur. Phys. J. A. 2007. V. 33. P. 223.
34. *Lukyanov V. K. et al.* // Ibid. V. 33. P. 389.
35. *Danilin B. V. et al.* // Phys. Rev. C. 2007. V. 76. P. 064612.
36. *Belyaev V. B., Tater M., Truhlik E.* // Ibid. V. 75. P. 034608.
37. *Kostyrykin V., Makarov K. A., Motovilov A. K.* // Trans. Amer. Math. Soc. 2007. V. 359. P. 77; *Albeverio S., Motovilov A. K., Selin A. V.* // SIAM J. Matrix Anal. Appl. 2007. V. 29. P. 685.
38. *Kartavtsev O. I., Malykh A. V.* // Pis'ma ZhETF. 2007. V. 86. P. 713; J. Phys. B. 2007. V. 40. P. 1429.
39. *Khvorostukhin A. S., Toneev V. D., Voskresensky D. N.* // Nucl. Phys. A. 2007. V. 791. P. 180.
40. *Titov A. I., Kampfner B.* // Phys. Rev. C. 2007. V. 76. P. 065211.
41. *Bondarenko S. et al.* // Phys. At. Nucl. 2007. V. 70. P. 2054.
42. *Ciofi degli Atti C. et al.* // Phys. Rev. C. 2007. V. 76. P. 055206.
43. *Poghosyan V. S. et al.* // Phys. Lett. B. 2008. V. 659. P. 768.
44. *Povolotsky A. M., Priezzhev V. B.* // J. Stat. Mech. 2007. P. P08018.
45. *Loutsenko I. M., Spiridonov V. P.* // SIGMA. 2007. V. 3. P. 059.
46. *Osipov V. A.* // J. Phys.: Condens. Matter. 2008. V. 20. P. 035204.
47. *Pepino R. T., Ferraz A., Kochetov E.* // Phys. Rev. B. 2008. V. 77. P. 013803.
48. *Chizhov A. V.* // JETP Lett. 2007. V. 85. P. 102.
49. *Plakida N. M., Oudovenko V. S.* // Physica C: Superconductivity. 2007. V. 460–462. P. 993.
50. *Shukrinov Yu. M., Mahfouzi F.* // Phys. Rev. Lett. 2007. V. 98. P. 157001.